

Khodayar Gholivand,<sup>a\*</sup> Hossein Mostaanzadeh,<sup>a</sup> Tomas Koval,<sup>b</sup> Michal Dusek,<sup>b</sup> Mauricio F. Erben<sup>c</sup> and Carlos O. Della Védova<sup>c,d\*</sup>

<sup>a</sup>Department of Chemistry, PO Box 14115-175, Faculty of Science, Tarbiat Modares University, Tehran, Iran, <sup>b</sup>Institute of Physics of the ASCR, v.v.i., Na Slovance 2, 182 21 Praha 8, Czech Republic, <sup>c</sup>CEQUINOR (UNLP-CONICET, CCT-La Plata), Departamento de Química, Facultad de Ciencias Exactas, Universidad Nacional de La Plata, CC 962, 47 esq. 115, (1900) La Plata, Argentina, and <sup>d</sup>Laboratorio de Servicios a la Industria y al Sistema Científico (UNLP-CIC-CONICET), Departamento de Química, Facultad de Ciencias Exactas, Universidad Nacional de La Plata, La Plata, Argentina

Correspondence e-mail:  
gholi\_kh@modares.ac.ir,  
carlosdv@quimica.unlp.edu.ar

# Synthesis, crystal structure and spectroscopic properties of a novel carbacylamidophosphate: *N*-(3-nitrobenzoyl)-*N'*,*N''*-bis(*tert*-butyl)phosphoric triamide

Received 25 February 2009  
Accepted 26 May 2009

The new compound *N*-(3-nitrobenzoyl)-*N'*,*N''*-bis(*tert*-butyl)phosphoric triamide was synthesized by reacting 3-nitrobenzoyl phosphoramidic dichloride and *tert*-butyl amine, and characterized by multinuclear (<sup>1</sup>H, <sup>13</sup>C and <sup>31</sup>P) NMR and FTIR spectroscopy techniques. Structural and conformational properties were analyzed using single-crystal X-ray diffraction, vibrational spectra and theoretical calculations. The crystal structure contains three symmetry-independent disordered molecules, connected *via* intermolecular N—H...O=P and N—H...O=C hydrogen bonds to form a centrosymmetric hexameric chain extended along the [2,1,1] direction. The disorder is mainly caused by rotation of the *tert*-butyl groups around the C—N bonds.

## 1. Introduction

Carbacylamidophosphate compounds with the general formula *R'*C(O)NHP(O)*R*<sub>2</sub> are attractive to study owing to their applications as *O*,*O'* donor ligands for metal complexation, particularly for lanthanide ions (Gubina & Amirkhanov, 2000; Skopenko *et al.*, 1996). Also their biological properties have been studied (Barak *et al.*, 2000; Mallender *et al.*, 2000), having a decisive role in catalytic and metabolism processes (Wu *et al.*, 2008; Schultz, 2003; Venkatachalam *et al.*, 2006). In the case of phosphoric triamide compounds, the three nitrogen subunits bonded to the phosphorus provide an opportunity for a large number of structurally diverse analogues and hence a broad spectrum of properties and shapes can be customized (Ishihara *et al.*, 1998; Verkade, 1993; Gholivand, Mostaanzadeh *et al.*, 2006). In previous works we discussed the structural properties of some of these molecules (Gholivand, Madani Alizadehgan *et al.*, 2006; Gholivand *et al.*, 2007; Gholivand, Della Védova *et al.*, 2008; Iriarte *et al.*, 2008; Gholivand, Pourayoubi *et al.*, 2005; Khodayar Gholivand, 2004; Gholivand, Shariatinia *et al.*, 2009), including cyclic variants containing the 1,3,2-diazaphospholidine-2,4,5-trione group (Gholivand, Oroujzadeh *et al.*, 2009). Moreover, a carbacylamidophosphate with two independent conformers in the unit cell has been reported (Gholivand & Pourayoubi, 2004).

Herein, the synthesis and spectroscopic characterization of *N*-(3-nitrobenzoyl)-*N'*,*N''*-bis(*tert*-butyl)phosphoric triamide is reported. The characterization of the novel compound was carried out by IR, <sup>1</sup>H, <sup>13</sup>C, <sup>31</sup>P NMR spectroscopy and elemental analysis. The molecular structure in the solid state has been determined by X-ray diffraction analysis. The experimental data were employed as references for quantum chemical calculations at the HF and B3LYP levels using the 6-31+G\* basis sets.

Table 1

Experimental details.

Crystal data	
Chemical formula	C <sub>90</sub> H <sub>150</sub> N <sub>24</sub> O <sub>24</sub> P <sub>6</sub>
<i>M<sub>r</sub></i>	2138.16
Crystal system, space group	Triclinic, <i>P</i> $\bar{1}$
Temperature (K)	120
<i>a</i> , <i>b</i> , <i>c</i> (Å)	13.1528 (2), 13.7179 (2), 16.5876 (2)
$\alpha$ , $\beta$ , $\gamma$ (°)	87.8019 (12), 70.8182 (13), 83.8446 (14)
<i>V</i> (Å <sup>3</sup> )	2810.41 (7)
<i>Z</i>	1
Radiation type	Mo <i>K</i> $\alpha$
$\mu$ (mm <sup>-1</sup> )	0.17
Crystal form, size (mm)	Irregular shape, 0.67 × 0.26 × 0.22
Data collection	
Diffractometer	Oxford Diffraction CCD
Data collection method	Rotation method data acquisition using $\omega$ scans
Absorption correction	Multi-scan†
<i>T<sub>min</sub></i>	0.945
<i>T<sub>max</sub></i>	0.963
No. of measured, independent and observed reflections	34 749, 11 679, 7286
Criterion for observed reflections	<i>I</i> > 3 $\sigma$ ( <i>I</i> )
<i>R<sub>int</sub></i>	0.028
$\theta_{max}$ (°)	26.5
Refinement	
Refinement on	<i>F</i>
<i>R</i> [ <i>F</i> <sup>2</sup> > 2 $\sigma$ ( <i>F</i> <sup>2</sup> )], <i>wR</i> ( <i>F</i> <sup>2</sup> ), <i>S</i>	0.042, 0.044, 1.79
No. of reflections	11 679
No. of parameters	679
H-atom treatment	Constrained to parent site
( $\Delta$ / $\sigma$ ) <sub>max</sub>	0.046
$\Delta\rho_{max}$ , $\Delta\rho_{min}$ (e Å <sup>-3</sup> )	0.37, -0.35

Computer programs used: *CrysAlis CCD* (Oxford Diffraction, 2007a), *CrysAlis RED* (Oxford Diffraction, 2007b), *SuperFlip* (Palatinus & Chapuis, 2007), *JANA2006* (Petricek *et al.*, 2006), *DIAMOND* (Brandenburg & Putz, 2004). † Based on symmetry-related measurements.

## 2. Experimental

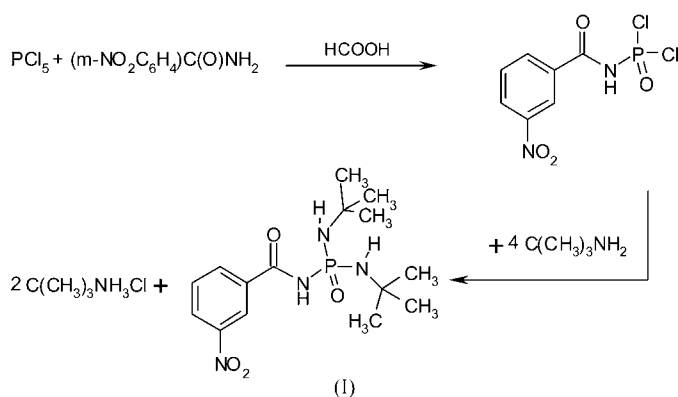
### 2.1. Materials and methods

All chemicals were purchased commercially and used without further purification. The melting point was determined on an Electrothermal apparatus. Elemental analysis was performed using a Heraeus CHN-O-RAPID instrument. <sup>1</sup>H, <sup>13</sup>C and <sup>31</sup>P NMR spectra were recorded on a Bruker (Avance DRS) 500 spectrometer. <sup>1</sup>H, <sup>13</sup>C and <sup>31</sup>P chemical shifts were determined relative to TMS and 85% H<sub>3</sub>PO<sub>4</sub>, respectively, as external standards. IR spectra (KBr pellets) were obtained with a Shimadzu, IR-60 model spectrometer. (*m*-NO<sub>2</sub>C<sub>6</sub>H<sub>4</sub>)C(O)N(H)P(O)Cl<sub>2</sub> was prepared similarly to the procedure reported by Kirsanov & Derkach (1956) from the reaction of phosphorus pentachloride and 3-nitrobenzamide followed by treatment with formic acid. X-ray diffraction data were measured with the four-circle diffractometer Gemini-Atlas of Oxford Diffraction.

### 2.2. Synthesis of (*m*-NO<sub>2</sub>C<sub>6</sub>H<sub>4</sub>)C(O)N(H)P(O)[NHC(CH<sub>3</sub>)<sub>3</sub>]<sub>2</sub>

Substituted phosphoramidic dichlorides and amines are ideal precursors for the preparation of carbacylamidophosphate species (Gubina & Amirkanov, 2000; Skopenko *et al.*,

1996; Gholivand, Alizadehgan *et al.*, 2006; Gholivand *et al.*, 2007; Gholivand, Della Védova *et al.*, 2008; Iriarte *et al.*, 2008; Gholivand, Pourayoubi *et al.*, 2005; Khodayar Gholivand, 2004; Gholivand, Shariatinia *et al.*, 2009). Thus, the title compound was synthesized by reacting 3-nitrobenzoyl phosphoramidic dichloride and *tert*-butyl amine, as shown in (I). To a solution of 3-nitrobenzoyl phosphoramidic dichloride (0.566 g, 2 mmol) in CH<sub>3</sub>CN (20 ml), a solution of *tert*-butyl amine (0.584 g, 8 mmol) in CH<sub>3</sub>CN (10 ml) was added dropwise at 273 K. After 24 h, the solvent was removed in vacuum and the solid was washed with distilled water. The residue was recrystallized in chloroform/acetonitrile (4:1) solution. Yield: 0.441 g (62%), m.p. 516 K. Anal.: calc. for C<sub>15</sub>H<sub>25</sub>N<sub>4</sub>O<sub>4</sub>P: C 50.6, H 7.0, N 15.7; found: C 50.74, H 6.90, N 15.46%. <sup>31</sup>P NMR (CDCl<sub>3</sub>, p.p.m.):  $\delta$  4.63 (br). <sup>13</sup>C NMR (CDCl<sub>3</sub>, p.p.m.):  $\delta$  31.48 [d, <sup>3</sup>*J*(P,C) = 5.0 Hz, CH<sub>3</sub>], 51.67 (s), 123.90 (s), 126.49 (s), 129.28 (s), 134.40 (s), 135.48 [d, <sup>3</sup>*J*(P,C) = 8.5 Hz, C<sub>ipso</sub>], 148.52 (s), 167.47 (s). <sup>1</sup>H NMR (CDCl<sub>3</sub>, p.p.m.):  $\delta$  1.30 (s, 18H), 3.25 [d, <sup>2</sup>*J*(PNH) = 6.9 Hz, 2H, NH<sub>amine</sub>], 7.61 [t, <sup>3</sup>*J*(H,H) = 8.0 Hz, 1H], 8.36 [dt, <sup>3</sup>*J*(H,H) = 8.1 Hz, <sup>5</sup>*J*(H,H) = 1.3 Hz, 1H], 8.68 [d, <sup>3</sup>*J*(H,H) = 7.7 Hz, 1H], 9.08 [t, <sup>5</sup>*J*(P,H) = 1.8 Hz, 1H], 10.82 (s, 1H, NH<sub>amide</sub>). IR (KBr, cm<sup>-1</sup>): 3320, 3070, 2950, 1648, 1524, 1447, 1344, 1228, 1192, 1019, 869, 801, 711.



### 2.3. Crystal structure determination

Single-crystal X-ray diffraction was carried out on a four-cycle diffractometer Gemini equipped with a CCD detector Atlas. Experimental details are given in Table 1.

A strong disorder was found for *tert*-butyl in the N—C(CH<sub>3</sub>)<sub>3</sub> group. The main task of the structure analysis was therefore to find an exact, reasonable and simple description of this phenomenon. Four ways are generally possible to describe disorder:

- by single atoms with large atomic displacement parameters (ADPs) described in harmonic approximation, *i.e.* with large displacement ellipsoids;
- by single atoms with anharmonic ADPs;
- by single atoms split to more positions, possibly bound with various constraints and restraints;
- by split rigid bodies.

A proper model should be selected with regard to the *R* value, goodness-of-fit, number of refined parameters and residual electron density in the difference-Fourier map.

**Table 2**

 Occupancies and rotation parameters for six N—C(CH<sub>3</sub>)<sub>3</sub> groups of the rigid-body model RB6.

 The coordinate system has been set up by the way that the  $\varphi$  angle defines rotation of *tert*-butyl along the corresponding N—C axis.

NoM <sup>†</sup>	N—C axis	NoS <sup>‡</sup>	$\varphi$ <sup>§</sup>	$\chi$ <sup>§</sup>	$\psi$ <sup>§</sup>	Occ1 <sup>¶</sup>
1	N3—C8	1	—	—	—	1
2	N4—C9	2	−32.1 (2)	−6.3 (3)	5.9 (7)	0.571 (3)
3	N7—C23	1	—	—	—	1
4	N8—C24	2	−42.22 (15)	4.0 (3)	5.8 (3)	0.420 (2)
5	N11—C38	2	−37.9 (2)	−2.6 (5)	8.4 (4)	0.519 (4)
6	N12—C39	2	−22.7 (4)	−9.8 (5)	−22.2 (4)	0.756 (3)

<sup>†</sup> NoM = sequence number of the source molecule. <sup>‡</sup> NoS = number of split positions of the source molecule. <sup>§</sup>  $\varphi$ ,  $\chi$  and  $\psi$  = rotation angles (°) transforming the first split position into the second one. <sup>¶</sup> Occ1 = occupancy of the first split position (the sum is 1 for each pair of split molecules).

In this case no indication of anharmonicity was found in the electron density maps. Therefore, we refined a structure model describing the disorder using method (i), *i.e.* using single atoms with large ADPs, hereinafter labeled the FAM (free atomic model). The FAM converged with  $R = 0.059$ , goodness-of-fit 4.36, and it contained 649 refined parameters.

The splitting of the positions of many disordered atoms would yield rather a confusing description so we have used rigid-body models instead. The program *JANA2006* (Petricek *et al.*, 2006) offers a variety of rigid-body descriptions, two of which were applicable to our structure:

(i) The rigid-body model RB1 contained one source molecule, N—C(CH<sub>3</sub>)<sub>3</sub>, with the coordinates and ADPs of all non-H atoms freely refined. The source molecule was transformed to six pairs of near positions in the elementary cell, thus creating six disordered *tert*-butyl groups. The total occupation of each pair was restricted to full occupation; the ratio of occupancies was refined. For each of the 12 positions we refined three components of the translation vector and three rotation angles  $\varphi$ ,  $\chi$  and  $\psi$ . The refinement converged with significantly worse reliability factors than FAM. However, this was caused by the common ADPs that were only refined for the source molecule being the same (except orientation) for all real positions in the elementary cell. After changing the refinement of ADPs to the TLS model, where the displacement parameters are refined independently for each transformed position as a rigid-group displacement, the results were better than those of FAM. RB1 finally converged with  $R_{\text{obs}} = 0.050$ , goodness-of-fit = 2.74, using 576 refined parameters.

(ii) In order to allow for a more flexible structure model we created the rigid-body model RB6 containing six source N—C(CH<sub>3</sub>)<sub>3</sub> groups (Table 2). As in RB1, the coordinates and ADPs of all the non-H atoms of the source molecules were freely refined. Using a translation vector and the rotation angles  $\varphi$ ,  $\chi$  and  $\psi$ , each of the six source molecules was transformed to two near positions, again creating six disordered fragments with restricted total occupancy and refined occupancy ratios. In RB6 the TLS description of the displacement parameters was not necessary. During the refinement

four rigid-body pairs were rotated in a way that splitting was clearly present, while two pairs merged into one position. Thus, in the final description we have four split N—C(CH<sub>3</sub>)<sub>3</sub> groups and two single molecules. RB6 converged with  $R_{\text{obs}} = 0.042$ , goodness-of-fit 2.25 and number of refined parameters 679, and it has been selected as the best description.

In order to understand the nature of the disorder we defined a coordinate system for RB6 in such a way that  $\varphi$  was always the rotation around the C—N axis. Table 2 shows that the amount of  $\varphi$  rotation dominates for all split positions. The disorder is therefore caused by the rotation of N—C(CH<sub>3</sub>)<sub>3</sub> groups around the C—N axis.

The structure was solved by a charge-flipping method using the program *SuperFlip* (Palatinus & Chapuis, 2007). The H atoms were localized from the difference-Fourier map. Whenever possible their coordinates were kept in an ideal geometry in the molecule. The N—H distances were restrained to 0.87 Å and the C—H distances to 0.96 Å. The isotropic temperature parameters of the H atoms were calculated as  $1.2U_{\text{eq}}$  of the parent atom.

#### 2.4. Computational methods

Quantum chemical calculations were performed with the *GAUSSIAN03* program package (Frisch *et al.*, 2003). Gradient techniques were used for the geometry optimizations and vibrational calculations. HF and B3LYP methods were employed with the standard 6-31+G\* Pople basis set. In addition, single-point calculations using a more extended basis set [6-311+G(2p,d)] were performed at the B3LYP level for all the stable conformers.

### 3. Results and discussion

#### 3.1. NMR studies

The <sup>31</sup>P{H} NMR spectrum exhibits a single peak at  $\delta = 4.63$  p.p.m. for the title compound. The <sup>1</sup>H NMR spectrum shows one single peak at  $\delta = 1.30$  p.p.m. for all the methyl protons and a doublet at  $\delta = 3.25$  p.p.m. for two aminic protons (<sup>2</sup> $J_{\text{PNH}} = 6.9$  Hz). An interesting point relating to the title compound is the coupling constant of <sup>5</sup> $J(\text{P,H}) \simeq 1.8$  Hz between the phosphorus and two aromatic protons, which is absent in many similar compounds. The <sup>13</sup>C NMR spectrum includes two doublet peaks for aliphatic and aromatic C atoms with <sup>3</sup> $J(\text{P,C}) = 5.0$  and 8.5 Hz, respectively.

#### 3.2. Structural analysis

The crystal structure of *N*-(3-nitrobenzoyl)-*N',N''*-bis(*tert*-butyl)phosphoric triamide consists of three symmetry-independent *a*, *b* and *c* molecules, distinguished by the different spatial orientations of the *tert*-butyl groups. Each form has N—C(CH<sub>3</sub>)<sub>3</sub> groups disordered by rotation around the C—N bonds. An *ORTEP* (Farrugia, 1997) drawing with atom numbering is shown in Fig. 1. A pronounced disorder described by split positions exists in one (out of two) *tert*-butyl amine of the *a* and *b* forms, and in both *tert*-butyl amines of *c*.

However, the atoms of non-split groups still have rather large ADPs, indicating that to some extent the disorder occurs for all *tert*-butyl groups.

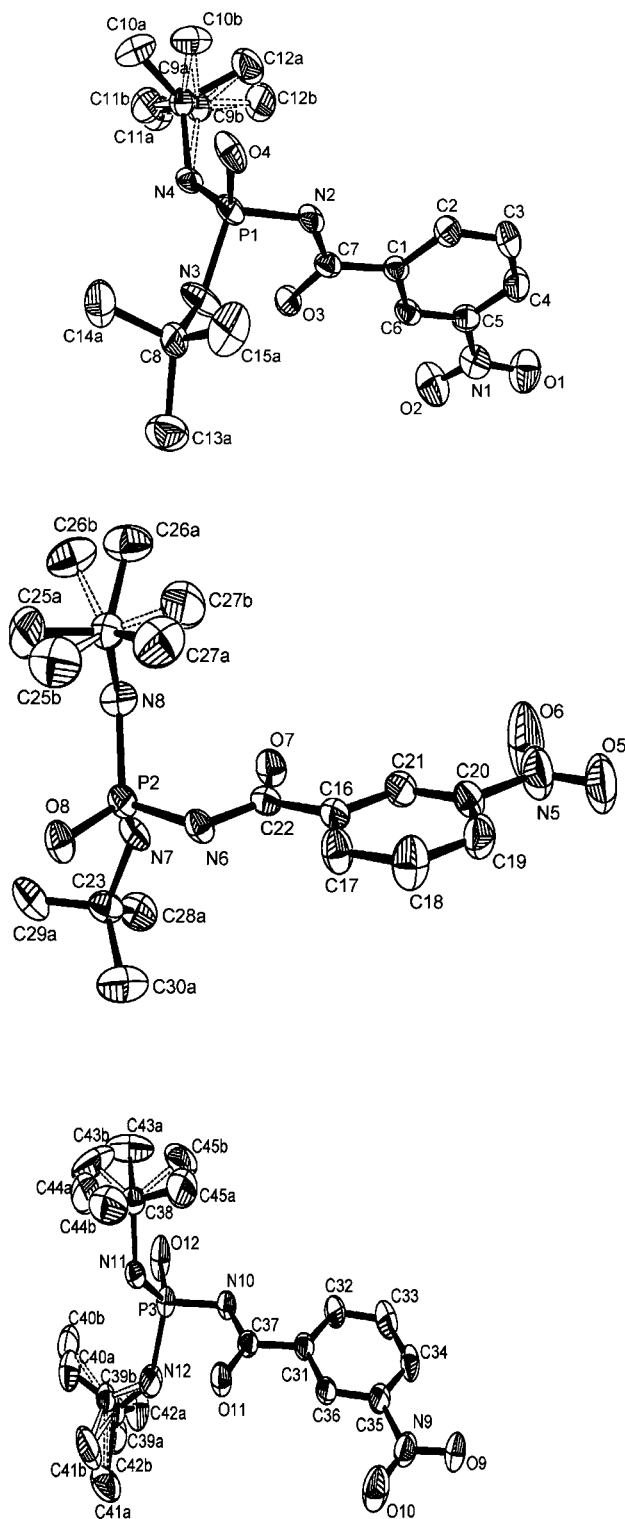


**Figure 1**  
Molecular structure and atom-labeling scheme for  $(3\text{-NO}_2\text{C}_6\text{H}_4)\text{-C}(\text{O})\text{NHP}(\text{O})[\text{NH}(t\text{-C}_4\text{H}_9)]_2$  showing three symmetry-independent disordered forms. The atoms are represented by 50% probability ellipsoids. H atoms have been omitted for clarity.

**Table 3**

Selected bond distances (Å) and angles (°) for the central moiety [see (II)] of *N*-(3-nitrobenzoyl)-*N',N''*-bis(*tert*-butyl)phosphoric triamide.

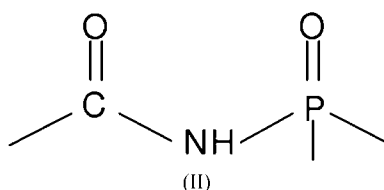
Parameter	X-ray	HF/6-31+G*	B3LYP/6-31+G
P=O	1.4720 (15)	1.464	1.493
P–N <sub>amine</sub>	1.6293 (17)	1.649	1.671
P–N <sub>amide</sub>	1.7053 (17)	1.717	1.751
C=O	1.2369 (19)	1.203	1.232
C–N <sub>amine</sub>	1.481 (3)	1.481	1.494
C–N <sub>amide</sub>	1.355 (3)	1.359	1.369
O=P–N <sub>amine</sub>	121.55 (9)	127.2	118.9
O=P–N <sub>amide</sub>	108.62 (9)	104.7	104.8
N <sub>amine</sub> –P–N <sub>amine</sub>	106.84 (9)	101.6	100.8
N <sub>amine</sub> –P–N <sub>amide</sub>	96.26 (8)	107.0	106.0
P–N <sub>amine</sub> –C	127.25 (15)	127.2	126.5
P–N <sub>amide</sub> –C	116.90 (16)	126.4	125.9
N–C=O	120.73 (16)	122.3	122.2

The crystal packing is dominated by the occurrence of P=O···H–N and C=O···H–N hydrogen bonds. Thus, the P1=O4···H2N–N2, C22=O7···H3N–N3, P2=O8···H10N–N10 and P3=O12···H6N–N6 hydrogen bonds form a centrosymmetric hexameric *CBAABC* chain in the crystalline lattice extended along the  $[2,1,\bar{1}]$  direction. In this chain the C=O···H–N hydrogen bonds are weaker than other hydrogen-bond interactions. Furthermore, there are intramolecular C=O···H–N<sub>amine</sub> hydrogen bonds in all three conformers (see Fig. 2). No hydrogen bonds were found to connect the chains in a three-dimensional network.

Selected geometrical parameters are given in Table 3. Geometrical parameters for each of the three symmetry-independent *a*, *b* and *c* forms are given in Table S1 of the supplementary information.<sup>1</sup> The phosphoryl and carbonyl groups are in an *anti* position to each other. This structural arrangement is typical for carbacylamidophosphate compounds containing the moiety shown in (II) (Gholivand *et al.*, 2007; Iriarte *et al.*, 2008; Gholivand, Della Védova *et al.*, 2005). The dihedral angles between the O=P double bond and the N–C amidic bond for *a*, *b* and *c* are 177.9 (9), 171.6 (9) and 179.6 (9)°, respectively. It is likely that the intermolecular hydrogen bond involving the carbonyl bond in *b* causes the small deviation from the local planarity observed for this form. Phosphorus assumes a slightly distorted tetrahedral configuration. The P=O bond lengths found in the molecules *a*, *b* and *c* are 1.4727 (15), 1.4774 (14) and 1.4656 (16) Å, which are larger than the normal P=O bond length (1.45 Å) found for example by Khodayar Gholivand (2004). All the P–N bonds in this compound are shorter than a typical P–N single bond (1.77 Å) and longer than a typical P=N double bond (1.57 Å; Corbridge, 1995). This is probably because of the overlap of the P–N sigma bond with the electrostatic effects of these polar bonds (Gilheany, 1994). It is

<sup>1</sup> Supplementary data, including H, <sup>13</sup>C and <sup>31</sup>P NMR, and FTIR spectra for the title compound are given in Figs. S1–7 and S8, respectively, selected geometrical parameters for each of the three symmetry-independent forms, for this paper are available from the IUCr electronic archives (Reference: BP5021). Services for accessing these data are described at the back of the journal.

interesting to note that in these conformers the form with the stronger P=O bond, *i.e.* *c*, has weaker P–N<sub>amine</sub> bonds, and the molecule with the weaker P=O bond, *i.e.* *a*, has stronger P–N<sub>amine</sub> bonds. The P–N<sub>amine</sub> and P–N<sub>amide</sub> bond lengths range between 1.623 (2)–1.633 (2) and 1.700 (2)–1.713 (2) Å (Table 3). Thus, the P–N amidic bond lengths are significantly longer than the P–N aminic ones. The sum of the surrounding angles for all the N atoms is almost 360°, therefore the environment of the N atoms is practically planar. As expected, the C–N amidic bond length was found to be shorter than the C–N single bond involving the amine groups; mean values: 1.355 (3) and 1.481 (3) Å for the C–N<sub>amine</sub> and C–N<sub>amide</sub> bond lengths.



To identify the effects of crystal packing on the molecular structure, quantum chemical calculations were performed for a molecule isolated in a vacuum. In the first step, the potential energy surface was analyzed to identify the different conformers. Three forms were obtained, depending on the mutual

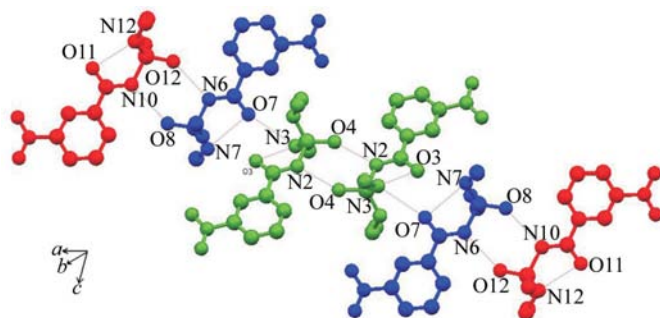


**Figure 2**  
View of the hydrogen bonding along the  $[2,1,1]$  direction in the crystal structure. The three symmetry-independent *a*, *b* and *c* forms are shown in green, blue and red, respectively. The dashed lines represent the hydrogen bonds. H atoms and methyl groups have been omitted for clarity.

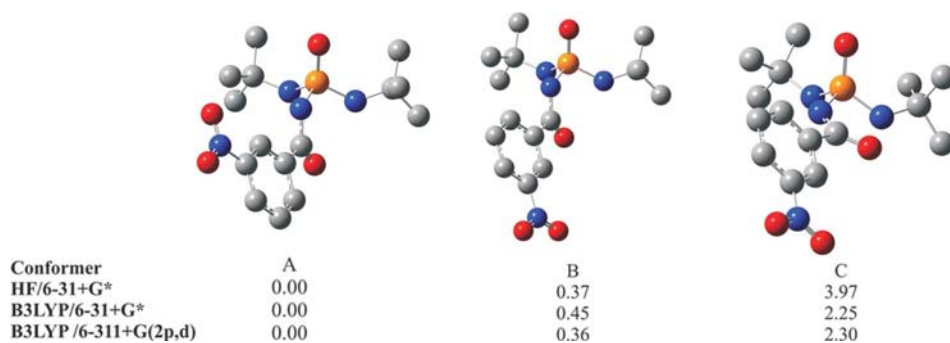


**Figure 3**  
Molecular structure of the main conformers found theoretically (B3LYP/6-31+G\*) for *N*-(3-nitrobenzoyl)-*N'*,*N''*-bis(*tert*-butyl)phosphoric triamide. H atoms have been omitted for clarity.

orientation of the 3-nitrobenzoyl group and the P=O double bond. These conformers are shown in Fig. 3. The *A* and *B* conformers have very similar electronic energies, the difference between them being lower than  $2.09 \text{ kJ mol}^{-1}$  for both HF and B3LYP levels of approximation. In these forms the P=O and C=O double bonds adopt a mutual *anti* position, the main difference between them is the relative orientation of the nitro and carbonyl groups in the nitrobenzoyl moiety. A third conformer, characterized by a non-planar local structure around the moiety shown in (II) is higher in energy. The three conformers have an alternate-like structure for the *tert*-butyl groups. The calculated second-most stable conformer *B* is structurally equivalent to the form observed in the crystalline state. Calculated (HF and B3LYP methods with 6-31+G\* basis sets) geometrical parameters (Table 3) are in moderate agreement with the experimental ones. The main differences are related to the N–P–N and P–N–C bond angles in the amide moiety, which are calculated *ca* 10° larger than those observed experimentally. The presence of intermolecular hydrogen bonds involving the amide group in the solid state could be responsible for these differences.

### 3.3. Vibrational spectra

The IR spectrum of the title compound (solid in KBr pellets) is given in the supplementary material and the most important absorptions, together with the computed vibrational data, are listed in Table 4. The harmonic vibrational frequencies were obtained for the fully optimized geometries of three conformers of the title compound. The importance of the vibrational analyses is twofold. First, it enables the characterization of a given conformation as a true minimum on the molecular potential energy surface. Secondly, if the conformation is confirmed to be a minimum, then the calculated harmonic frequencies are useful in the assignment of the experimental vibrational data. Thus, a tentative assignment of the observed bands was carried out by comparison with theoretical wavenumbers, as well as with the relevant data reported in the literature for related molecules (Gholivand, Della Védova *et al.*, 2005; Gholivand, Alizadehgan *et al.*, 2006; Gholivand *et al.*, 2007; Gholivand, Della Védova *et al.*, 2008; Iriarte *et al.*, 2008; Gholivand, Madani Alizadehgan *et al.*, 2008; Gholivand, Pourayoubi *et al.*, 2005; Khodayar Gholivand, 2004; Gholivand, Shariatnia *et al.*, 2009). The main features in the vibrational spectra can be satisfactorily interpreted on the basis of the presence of the *B* form in the solid.

The IR spectrum for the title compound shows the presence of three well defined absorptions in the high-frequency range at 3320, 3070 and 2950  $\text{cm}^{-1}$ . The former band is assigned to the N–H stretching mode of the amide

**Table 4**

Selected experimental and calculated vibrational data ( $\text{cm}^{-1}$ ) for *N*-(3-nitrobenzoyl)-*N'*,*N''*-bis(*tert*-butyl)phosphoric triamide.

Experimental <sup>†</sup>	Calculated <sup>‡</sup>	Tentative assignment
3320 s	3595	$\nu(\text{N}-\text{H})_{\text{amide}}$
3070 s	3564	$\nu(\text{N}-\text{H})_{\text{amine}}$
2950 s	3478	$\nu(\text{N}-\text{H})_{\text{amine}}$
1648 vs	1721	$\nu(\text{C}=\text{O})$
1608 w	1666	$\nu(\text{C}=\text{C})_{\text{ring}}$
1576 w	1629	
1524 vs	1606	$\nu_{\text{as}}(\text{NO}_2)$
1447 vs	1445	$\delta(\text{N}-\text{H})_{\text{amide}}$
1413 m	1436	$\delta(\text{N}-\text{H})_{\text{amine}}$
	1430	
1344 vs	1385	$\nu(\text{C}-\text{NO}_2)$
1228 s	1285	$\nu(\text{P}=\text{O})$
1192 vvs	1262 <sup>§</sup>	$\nu(\text{C}-\text{C})_{\text{tert-butyl}}$
	1260	
	1254	
	1247	
1039 s	1149	$\nu(\text{C}-\text{N})_{\text{amide}}$
1019 s	1019	$\nu(\text{P}-\text{N})_{\text{amine}}$
	998	
916 w	998	$\rho_{\text{s}}(\text{N}-\text{H})$
869 m	871	$\nu(\text{P}-\text{N})_{\text{amide}}$
801 m	856	$\delta(\text{CH}_3)$
711 m	792	$\rho(\text{C}-\text{H})_{\text{ring}}$
570 w	634	$\rho(\text{N}-\text{H})$

<sup>†</sup> Solid in KBr pellets. <sup>‡</sup> B3LYP/6-31+G\* method without factor scale correction. <sup>§</sup> Most intense absorptions calculated for the  $\nu(\text{C}-\text{C})_{\text{tert-butyl}}$  modes.

group, whereas the latter are due to similar modes in the amine groups. The strong intensity bands centered at 1648 and 1524  $\text{cm}^{-1}$  can be assigned with confidence to stretching vibrations of the carbonyl and nitro [ $\nu_{\text{as}}(\text{NO}_2)$ ] groups, respectively. Two strong absorptions centered at 1228 and 1192  $\text{cm}^{-1}$  appear overlapped, the first can be assigned with confidence to the  $\text{P}=\text{O}$  stretching mode, while several  $\nu(\text{C}-\text{C})$  stretching modes in the *tert*-butyl groups are also expected to occur in this region. Other characteristic fundamentals for carbacylamidophosphate species are the  $\text{N}-\text{C}$  and  $\text{N}-\text{P}$  stretching modes, typically observed in the 1100–800  $\text{cm}^{-1}$  region (Gholivand, Alizadehgan *et al.*, 2006; Gholivand *et al.*, 2007; Gholivand, Della Védova *et al.*, 2008; Iriarte *et al.*, 2008; Gholivand, Pourayoubi *et al.*, 2005; Khodayar Gholivand, 2004; Gholivand, Shariatinia *et al.*, 2009). In the present case the  $\nu(\text{C}-\text{N})_{\text{amide}}$  fundamental is located at 1039  $\text{cm}^{-1}$ . It is also interesting to note that the  $\nu(\text{P}-\text{N})_{\text{amine}}$  mode at 1019  $\text{cm}^{-1}$  appears at higher frequencies than the corresponding mode of the amidic nitrogen at 869  $\text{cm}^{-1}$  [ $\nu(\text{P}-\text{N})_{\text{amide}}$ ]. Calculated B3LYP/6-31+G\* values are 1019 and 998, and 871  $\text{cm}^{-1}$  for the  $\nu(\text{P}-\text{N})_{\text{amine}}$  and  $\nu(\text{P}-\text{N})_{\text{amide}}$  modes, respectively, in good agreement with the experimental data.

#### 4. Conclusions

*N*-(3-Nitrobenzoyl)-*N'*,*N''*-bis(*tert*-butyl)phosphoric triamide was prepared in good yield and purity by treating 3-nitrobenzoyl phosphoramidic dichloride with *tert*-butyl amine. The novel species was characterized by multinuclear ( $^1\text{H}$ ,  $^{13}\text{C}$  and  $^{31}\text{P}$ ) NMR and FTIR spectroscopy techniques. Structural properties were determined using vibrational spectroscopy as

well as X-ray diffraction analysis. It is apparent that phosphoric triamides substituted with *tert*-butyl groups have strongly disordered structures in the crystal (Khodayar Gholivand, 2004). X-ray crystallography has confirmed the presence of three symmetry-independent forms of the molecule. The carbacylamidophosphate shown in (II) moiety shows well defined structural and spectroscopic features (Gholivand, Shariatinia *et al.*, 2009).

The financial support of this work by the Research council of Tarbiat Modares University is gratefully acknowledged. We also thank the Grant Agency of the Czech Republic, project No. 202/06/0757. We also thank Karla Fejfarova from the Institute of Physics for technical help with CIF preparation. The Argentinean authors thank the Consejo Nacional de Investigaciones Científicas y Técnicas (CONICET), the Comisión de Investigaciones Científicas de la Provincia de Buenos Aires (CIC), the Facultad de Ciencias Exactas, Universidad Nacional de La Plata, República Argentina for financial support. CODV especially acknowledges the DAAD for its generous sponsorship of the DAAD Regional Program of Chemistry of the Republic of Argentina (supporting Latin-American students for a PhD program in La Plata).

#### References

- Barak, D., Ordentlich, A., Kaplan, D., Barak, R., Mizrahi, D., Kronman, C., Segall, Y., Velan, B. & Shafferman, A. (2000). *Biochemistry*, **39**, 1156–1161.
- Brandenburg, K. & Putz, H. (2004). *DIAMOND*, Version 3. University of Bonn, Germany.
- Corbridge, D. E. C. (1995). *Phosphorus: An Outline of Its Chemistry, Biochemistry and Technology*, 5th Ed. Amsterdam: Elsevier.
- Farrugia, L. J. (1997). *J. Appl. Cryst.* **30**, 565.
- Frisch, M. J. *et al.* (2003). *GAUSSIAN03*, Revision B.04. Gaussian Inc., Pittsburgh PA.
- Gholivand, K., Alizadehgan, A. M., Arshadi, S. & Firooz, A. A. (2006). *J. Mol. Struct.* **791**, 193–200.
- Gholivand, K., Della Védova, C. O., Anaraki Firooz, A., Madani Alizadehgan, A., Michelini, M. C. & Pis Diez, R. (2005). *J. Mol. Struct.* **750**, 64–71.
- Gholivand, K., Della Védova, C. O., Erben, M. F., Mahzouni, H. R., Shariatinia, Z. & Amiri, S. (2008). *J. Mol. Struct.* **874**, 178–186.
- Gholivand, K., Della Védova, C. O., Erben, M. F., Mojahed, F. & Alizadehgan, A. M. (2007). *J. Mol. Struct.* **840**, 66–70.
- Gholivand, K., Madani Alizadehgan, A., Mojahed, F. & Soleimani, P. (2008). *Polyhedron*, **27**, 1639–1649.
- Gholivand, K., Mostaanzadeh, H., Shariatinia, Z. & Oroujzadeh, N. (2006). *Main Group Chem.* **5**, 95–109.
- Gholivand, K., Oroujzadeh, N., Erben, M. F. & Della Védova, C. O. (2009). *Polyhedron*, **28**, 541–547.
- Gholivand, K. & Pourayoubi, M. (2004). *Z. Anorg. Allg. Chem.* **630**, 1330–1335.
- Gholivand, K., Pourayoubi, M., Shariatinia, Z. & Mostaanzadeh, H. (2005). *Polyhedron*, **24**, 655–662.
- Gholivand, K., Shariatinia, Z., Mashhadi, S. M., Daepour, F., Farshidnasab, N., Mahzouni, H. R., Taheri, N., Amiri, S. & Ansar, S. (2009). *Polyhedron*, **28**, 307–321.
- Gilheany, D. G. (1994). *Chem. Rev.* **94**, 1339–1374.
- Gubina, K. E. & Amirkhanov, V. M. (2000). *Z. Naturforsch. B*, **55**, 1015–1019.
- Iriarte, A. G., Erben, M. F., Gholivand, K., Jios, J. L., Ulic, S. E. & Della Védova, C. O. (2008). *J. Mol. Struct.* **886**, 66–71.

- Ishihara, K., Karumi, Y., Kondo, S. & Yamamoto, H. (1998). *J. Org. Chem.* **63**, 5692–5695.
- Kirsanov, A. V. & Derkach, G. I. (1956). *Zh. Obshch. Khim.* **26**, 2082.
- Mallender, W. D., Szegletes, T. & Rosenberry, T. L. (2000). *Biochemistry*, **39**, 7753–7763.
- Oxford Diffraction (2007a). *CrysAlis CCD*. Oxford Diffraction, Abingdon, Oxfordshire, England.
- Oxford Diffraction (2007b). *CrysAlis RED*. Oxford Diffraction, Abingdon, Oxfordshire, England.
- Palatinus, L. & Chapuis, G. (2007). *J. Appl. Cryst.* **40**, 786–790.
- Petricek, V., Dusek, M. & Palatinus, L. (2006). *JANA2006*. Institute of Physics, Prague, Czech Republic.
- Schultz, C. (2003). *Bioorg. Med. Chem.* **11**, 885–898.
- Skopenko, V. V., Amirkhanov, V. M., Ovchinnikov, V. A. & Turov, A. V. (1996). *Russ. J. Inorg. Chem.* **41**, 589.
- Venkatachalam, T. K., Sarquis, M., Qazi, S. & Uckun, F. M. (2006). *Bioorg. Med. Chem.* **14**, 6420–6433.
- Verkade, J. G. (1993). *Acc. Chem. Res.* **26**, 483–489.
- Wu, L. Y., Do, J. C., Kazak, M., Page, H., Toriyabe, Y., Anderson, M. O. & Berkman, C. E. (2008). *Bioorg. Med. Chem. Lett.* **18**, 281–284.